Int. J. Heat Mass Transfer. Vol. 30, No. 10, pp. 2023–2030, 1987
Printed in Great Britain

0017–9310/87 $3.00 + 0.00

Conventional and conditional Prandtl number in a turbulent plane wake

R. A. ANTONIA and L. W. B. BROWNE
Department of Mechanical Engineering, University of Newcastle, N.S.W., 2308, Australia

(*Received* 4 *September* 1985 *and in final form* 2 *September* 1986)

Abstract—Conventional and conditional measurements of several turbulence quantities and particularly of the turbulent Prandtl number are presented for the nearly self-preserving region of a slightly heated wake of a circular cylinder. To verify that the measurements were made in the self-preserving region, and to also serve as a check on measurement accuracy, three stations in the wake were used. The identification of the turbulent regions in the outer part of the wake was based on the behaviour of the probability density function of the temperature fluctuation. Conventional distributions of the turbulent diffusivities of momentum and heat vary considerably in the outer part of the wake. This variation is not reduced when only turbulent zone averages are considered. The turbulent Prandtl number varies significantly in the turbulent part of the flow.

INTRODUCTION

ALTHOUGH several detailed measurements [1–7] have been made of various aspects of the turbulent wake of a heated two-dimensional cylinder, there is relatively little information available to permit a reliable quantitative comparison to be made between the momentum and heat transport characteristics of this flow. In particular, accurate values of the turbulent Prandtl number across the wake have not yet been determined. In the sense that Pr_T is a quantitative indicator of the relative strengths of momentum and heat transports, an accurate knowledge of the variation of Pr_T is important, especially for testing heat transport models.

The aim of the present study was to accurately determine distributions of $\overline{uv}$ and $\overline{v\theta}$ in the self-preserving region of a wake with a view to determining a sufficiently accurate distribution for the turbulent Prandtl number. As in the study of Fabris [7], both conventional and conditional measurements were made but over a wider range of x/d (270–600) than considered by Fabris. These measurements permit estimates to be made of Pr_T on a conventional basis and, by focusing on only the turbulent region of the flow, an estimate of Pr_T on a conditional basis.

EXPERIMENTAL TECHNIQUES

A non-return blower-type wind tunnel with a working section 350 × 350 mm, 2.4 m long was used. The wake was generated by a stainless steel cylindrical tube of 2.67 mm o.d. (d) mounted horizontally in the mid-plane of the working section, 20 cm after the end of the wind tunnel contraction. The floor of the working section was slightly tilted to maintain a zero pressure gradient in the working section. All measurements were made at a nominal free stream velocity U_1 of 6.7 m s^{-1} ($U_1 d/\nu \simeq 1190$) and at three streamwise stations; $x/d = 270$, 420 and 600. The stainless steel tube was heated electrically, the amount of heat used being sufficiently small for temperature to be a passive marker of the flow.

The velocity fluctuations u and v were measured with an X-probe. The X-probe hot wires (Pt–10% Rh) had a diameter of 5 μm, a length of about 1 mm and were separated in the z-direction by about 0.9 mm. The wires were operated at an overheat ratio of 1.8 in DISA 55M10 constant temperature circuits. For the measurement of the temperature fluctuation θ, a cold wire (Pt–10% Rh) of diameter $d_w \simeq 0.63$ μm was operated in a constant current (0.1 mA) circuit. This wire was aligned in the z-direction and placed 0.5 mm in front of the wire crossing point of the X-probe. The cold wire length ($l_w \simeq 1$ mm) was sufficient to avoid any possible interference of the wakes from the cold wire stubs (unetched parts of the Wollaston wire) with the hot wires. Another important consideration in choosing the wire length was the need to minimize the end conduction effect (e.g. Paranthoen *et al.* [8]) whilst keeping the attenuation at the high frequency end of the temperature spectrum as small as possible. Experiments carried out (details will be reported elsewhere) with a wide range of wire lengths indicated that, for this particular flow, no significant reduction in $\overline{\theta^2}$ could be discerned for wires in the range $1500 < l_w/d_w < 2600$. The wire which was used ($l_w/d_w \simeq 1600$) meets this criterion. For this wire the ratio l_w/l_K was in the range 1.4–2.4 over the wake cross-section. We also found that it was important to locate the cold wire at a relatively small distance upstream of the X-probe in order not to degrade the correlation between u and θ. Further details are given in ref. [9]. The X-probe, with the cold wire in its final location, was calibrated in the free stream for velocity

NOMENCLATURE

b $(U_1/U_0)\,dL/dx$
d cylinder diameter [m]
d_w cold wire diameter [m]
I intermittency function: 1, in turbulent region; 0, in non-turbulent region
l_K Kolmogorov length scale, $(\nu^3/\bar{\varepsilon})^{1/4}$ [m]
l_w cold wire length [m]
L mean velocity defect half-width [m]
p_θ probability density function of θ
P_θ cumulative probability of θ
Pr_T turbulent Prandtl number, ν_T/α_T
$\bar{T}$ mean temperature, relative to ambient [°C]
T_0 maximum mean temperature excess at wake centreline [°C]
$\bar{U}$ mean velocity in x-direction [m s^{-1}]
U_0 maximum mean velocity defect at wake centreline [m s^{-1}]
$\overline{uv}$ conventional kinematic Reynolds shear stress [m^2 s^{-2}]
u, v, w velocity fluctuations in x-, y- and z-directions, respectively ($\bar{u} = \bar{v} = \bar{w} = 0$) [m s^{-1}]
$\bar{V}$ mean velocity in y-direction [m s^{-1}]
$\overline{v\theta}$ conventional (thermometric) lateral heat flux [m s^{-1} °C]
x longitudinal direction with origin at the centre of the cylinder [m]
x_0 effective or virtual origin [m]
y direction of main shear, with origin at the centreplane of the wake [m]
z spanwise direction, with origin at the centreplane of the wake [m].

Greek symbols
α thermal diffusivity [m^2 s^{-1}]
α_T turbulent diffusivity of heat [m^2 s^{-1}]
γ intermittency factor $\equiv \bar{I}$
$\bar{\varepsilon}$ average turbulent energy dissipation [m^2 s^{-3}]
η non-dimensional distance, y/L
θ temperature fluctuation ($\bar{\theta} = 0$) [°C]
ν kinematic viscosity [m^2 s^{-1}]
ν_T turbulent diffusivity of momentum [m^2 s^{-1}].

Subscripts and other symbols
1 refers to free stream
$\bar{(\ )}$ denotes conventional average $\equiv T^{-1}\int_0^T (\ )\,dt$
$\bar{(\ )}_t$ denotes averaging in the turbulent region of the flow only, $(\gamma T)^{-1}\int_0^T I(\ )\,dt$.

and yaw ($\pm 12°$). The temperature coefficient of the 0.63 μm cold wire ($\simeq 1.69 \times 10^{-3}$ °C^{-1}) was determined with the latter mounted in the exit plane of a heated circular jet over a range of temperatures covering that used in the experiment. The mean temperature of the jet was measured with a Pt-resistance thermometer (Leeds & Northrup) capable of resolving 0.01°C.

The output voltages from the DISA 55M10 bridges and the constant current circuit were digitized, after suitable offset and gain, on-line to a PDP 11/34 computer at a sampling frequency of 2 kHz after filtering at a cut-off frequency of 1 kHz. The time series of voltages were converted to time series of velocity (u, v) and temperature using the appropriate calibrations for velocity and temperature of the hot and cold wires. A total record duration of 50 s was sufficient to ensure convergence of conventional averages at all values of y. To ascertain that convergence had been achieved, the averages were computed for increasingly longer portions of the total record. For example, the final values of $\overline{uv}$, $\overline{u\theta}$ and $\overline{v\theta}$ were achieved to within $\pm 2\%$ for durations typically equal to about half the total record duration. At $\eta = 2.1$ ($\gamma \simeq 0.10$), the final values of $(\overline{uv})_t$, $(\overline{u\theta})_t$ and $(\overline{v\theta})_t$ were achieved only to within $\pm 10\%$ at approximately half the total record duration, emphasizing the slower convergence of conditional averages near the edge of the wake.

The two-dimensionality of the flow was checked by measuring the correlation coefficient between u and w across the wake with the X-wire in the x–z plane. Both conventional and conditionally turbulent values of this coefficient were generally smaller than 0.1, providing reasonable support for two-dimensionality. Another check of two-dimensionality was provided by the negligible dependence on z of the distributions of the intermittency factor γ in the intermittent region of the flow. This check is similar to that made by Barsoum *et al.* [10] in the near wake ($x/d \simeq 96$) of a circular cylinder.

DETECTION OF INTERMITTENCY

The detection of the turbulent/non-turbulent interface was made on the basis of the temperature fluctuation. The difficulties in obtaining an unambiguous detection are well known (e.g. Antonia [11]) and need not be discussed here. The present approach, like that of Bilger *et al.* [12], is based on the shape of the probability density function (pdf) of θ near the ambient temperature level of the free stream. In the absence of free stream temperature fluctuations and electronic noise we would expect a Dirac delta function for that part of the pdf. A cumulative probability distribution of θ, such as shown in Fig. 1, should then asymptote to a vertical line at $(1-\gamma)$. This is not observed in Fig. 1. Since the free stream temperature fluctuations and electronic noise are, to a reasonable approximation,

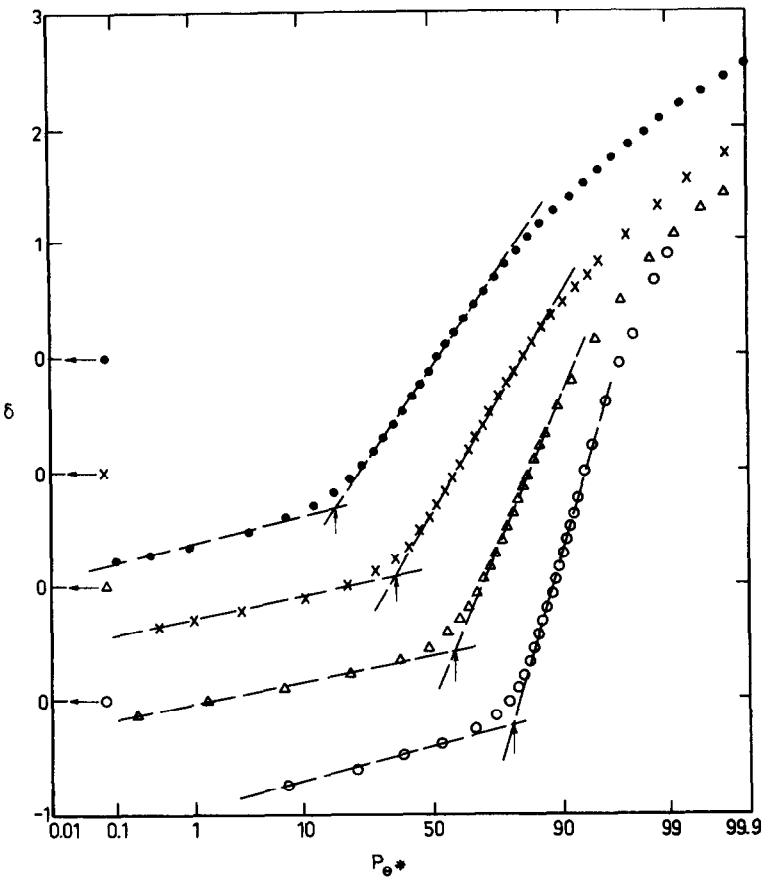

FIG. 1. Cumulative probability distributions of temperature at four locations in the wake at $x/d = 420$. Note the displacement in the origin for the ordinate.

Gaussianly distributed, the cumulative probability follows a straight line as the temperature approaches the ambient value. A departure from this line should indicate the entry into the turbulent region. Denoting by δ the variable in probability space taken by the physical variable θ^* (the asterisk denotes normalization by the r.m.s. value), the cumulative probability of θ^* is given by

$$P_{\theta^*} = \int_{\delta_a}^{\delta} p_{\theta^*}\, \mathrm{d}\delta.$$

The pdf of θ^* is zero at $\delta = \delta_a$, corresponding approximately to the ambient temperature. The distributions of P_{θ^*}, shown in Fig. 1 at four values of η, approximately follow, at the smallest values of δ, the linear behaviour described above. As δ increases, P_{θ^*} tends to follow another straight line. A further departure from this second line occurs at large values of δ, with P_{θ^*} in excess of about 0.9. The intermittency factor γ is assumed equal to $1 - P_c$, where P_c is the probability at the intersection of the two lines in Fig. 1. The intermittency function was generated by choosing the threshold level at the value of θ^* on the probability curve which corresponds to P_c.

The resulting distributions of γ, shown on probability paper in Fig. 2, are consistent with self-preservation. These distributions are approximately linear

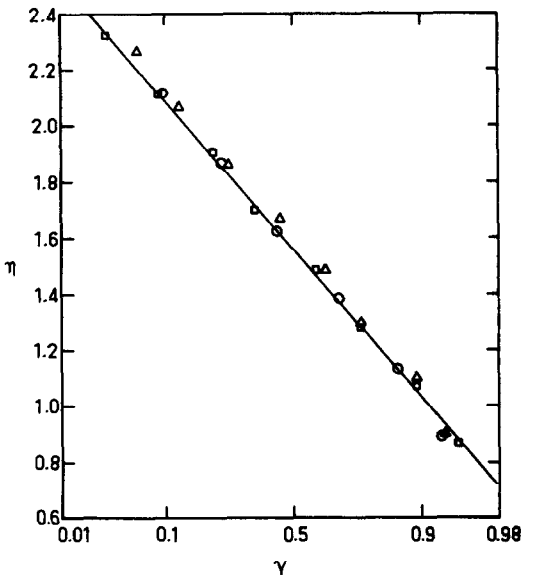

FIG. 2. Distributions of the intermittency factor: △, $x/d = 273$; ○, 420; □, 600; ——, Gaussian distribution.

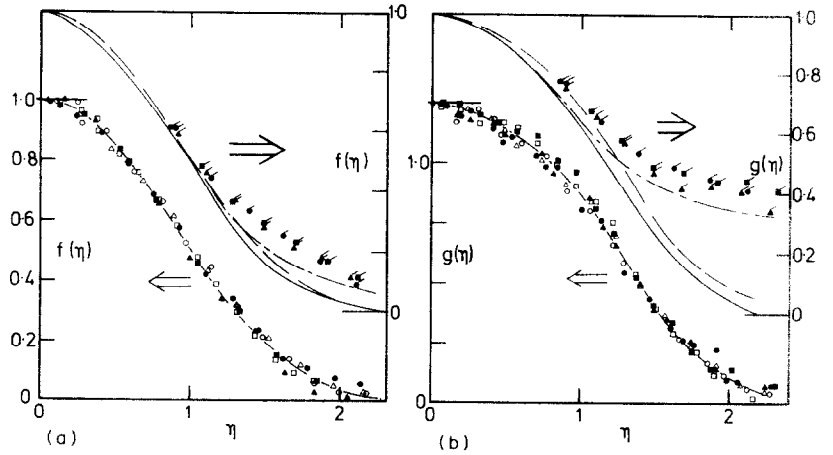

FIG. 3. Mean velocity and mean temperature distributions: (a) mean velocity; (b) mean temperature. Conventional data: △, $x/d = 273$; ○, 420; □, 600 (to indicate flow symmetry about the centreline, data obtained for $\eta < 0$ are shown as closed symbols); ——, best fit to conventional data. Turbulent zone averages (note vertical shift in the ordinate): ◭, $x/d = 273$; ◉, 420; ■, 600. Fabris [7]: ——, conventional; ——·——, turbulent zone averages.

suggesting that the pdf of the turbulent/non-turbulent interface is nearly Gaussian. The straight line in Fig. 2, which is a best fit to the data, indicates that the mean position of the interface is at $\eta \simeq 1.60$ and its standard deviation is about $0.4L$. Using Fabris' [13] distributions for γ at $x/d = 400$, we estimate mean and r.m.s. values of the interface of $1.63L$ and $0.34L$, respectively. This comparison is favourable.

RESULTS AND DISCUSSION

Conventional mean velocity and mean temperature distributions measured at the three streamwise stations (Fig. 3) are in good agreement with the assumption of self-preservation. These measurements were carried out separately using a total head tube for velocity and a single cold wire for temperature, details of which are given in ref. [9]. In Fig. 3(a), $f(\eta)$ is the normalized velocity defect $(U_1 - \bar{U})/U_0$ and, in Fig. 3(b), $g(\eta)$ is the normalized temperature excess $\bar{T}/T_0$. The scatter in the data for $g(\eta)$ is larger than for $f(\eta)$. To avoid confusion with the conventional data, a shift in the vertical origin is used in Fig. 3 to present the turbulent zone averaged data. Least squares best fit curves for the conventional data are reproduced, using the shifted ordinate, for comparison with the conditional data. Like the conventional data, the conditional data are in good agreement with self-preservation. This result follows from the well-established relations [14], e.g.

$$\bar{U} = \gamma \bar{U}_t + (1-\gamma) U_1$$

$$\bar{T} = \gamma \bar{T}_t$$

and the previously observed self-preserving forms for f, g and the intermittency factor γ.

The difference between g_t and g for $\eta > 1$ is significantly larger than that between f_t and f. This difference has been noted in other turbulent shear flows such as a boundary layer and plane and circular jets. It has also been observed in the near wake of a flat plate by Ali and Kovasznay [15]. The distributions of ref. [13] (Fig. 3) at $x/d = 400$ also highlight this difference. In particular, both the present and Fabris' distributions for g_t tend towards a constant at large values of η, emphasizing the uniformity of the mean temperature within turbulent bulges. The difference between the shapes of distributions of mean velocity and mean temperature across the wake is further underlined when considering gradients with respect to η of f (or f_t) and g (or g_t). Whereas f' ($\equiv \partial f/\partial\eta$) monotonically increases between zero at $\eta = 0$ to a maximum near $\eta = 1$ (Fig. 4), g' tends to flatten out, almost exhibiting a point of inflection near $\eta = 0.5$, before reaching a maximum near $\eta \simeq 1.2$. This inflectional behaviour is more pronounced on the mean temperature profile in a mixing layer (e.g. ref. [16]) where it has been associated with the coherent large-scale motion.

Conventional and conditional averages of the products uv and $v\theta$ are shown in Figs. 5(a) and (b), respectively. For the turbulent conditional averages, averages of fluctuations in only the turbulent zones were subtracted from the instantaneous conventional fluctuations before forming the products. In our definition, which corresponds to 'z-averaging' in Fabris' [7] terminology, $\overline{(uv)}_t \equiv \overline{[(u-\bar{u}_t)(v-\bar{v}_t)]}_t$ and $\overline{(v\theta)}_t = \overline{[(v-\bar{v}_t)(\theta-\bar{\theta}_t)]}_t$. Had overall means been used instead of zone averaged means, the corresponding fluxes would be $\overline{(uv)}_t + \bar{u}_t\bar{v}_t$ and $\overline{(v\theta)}_t + \bar{v}_t\bar{\theta}_t$. We have chosen to use $\overline{(uv)}_t$ and $\overline{(v\theta)}_t$ as these definitions are in closest analogy to the conventional averages $\overline{uv}$ and $\overline{v\theta}$.

The conventional and conditional data in Fig. 5 provide good support for the concept of self-preservation. The scatter in the values of $\overline{(uv)}_t$ and $\overline{(v\theta)}_t$ at large values of η is of the same order as that in $\overline{uv}$ and $\overline{v\theta}$, providing indirect support for the adequacy of the

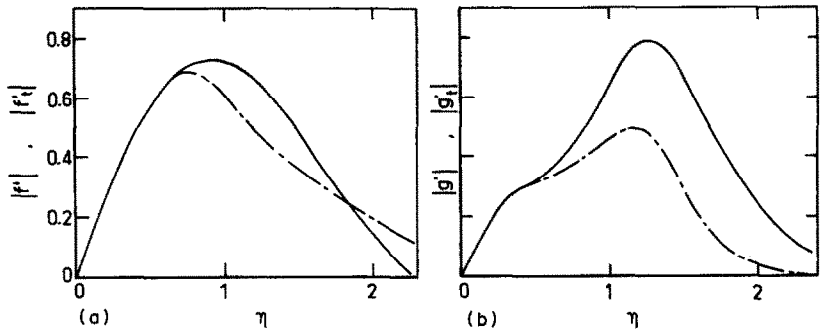

FIG. 4. Derivatives with respect to η of the mean velocity and temperature distributions: (a) mean velocity derivatives; (b) mean temperature derivatives. ——, Conventional; ——·——, turbulent zones.

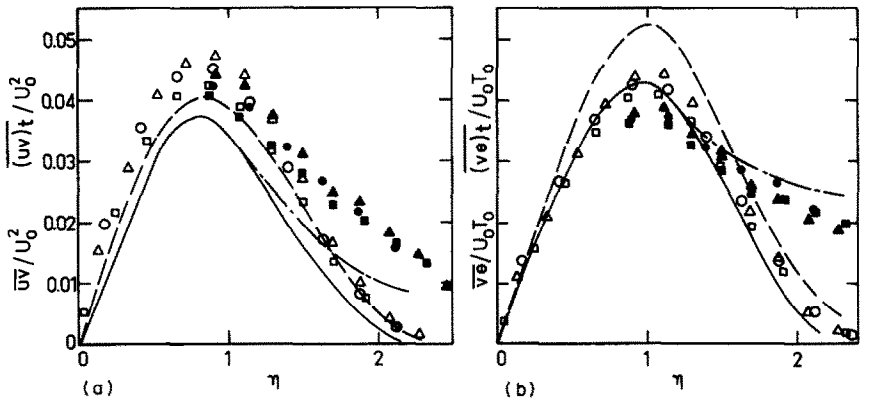

FIG. 5. Reynolds shear stress and lateral heat flux distributions: △, $x/d = 273$; ○, 240; □, 600. Open symbols designate conventional values. Closed symbols designate values in turbulent zones. ——, Calculated using equations (1) and (2). Fabris [7]: ——, conventional; ——·——, turbulent zones.

duration of the digital recordings. As expected, there is a significant difference between conditional and conventional averages. There is also a tendency for $\overline{(v\theta)_t}$ to approach a constant value at large η, in analogy with the trend shown by $\bar{T}_t$. Fabris' distributions (Fig. 5(b)) of $\overline{v\theta}$ and $\overline{(v\theta)_t}$ are in reasonable agreement with the present values. His distribution of $\overline{uv}$ is however smaller than the present distribution; the difference between his $\overline{uv}$ and $\overline{(uv)_t}$ distributions is also smaller than the present difference. It is difficult to provide a rational explanation for these differences. The distributions of $\overline{uv}$ and $\overline{v\theta}$ were calculated using the mean momentum and mean enthalpy equations and the measured mean velocity and mean temperature profiles. Assuming self-preservation, the calculated distributions of $\overline{uv}$ and $\overline{v\theta}$ are given by (e.g. Tennekes and Lumley [17])

$$\frac{\overline{uv}}{U_0^2} = -bf\eta \tag{1}$$

and

$$\frac{\overline{v\theta}}{U_0T_0} = bg\eta \tag{2}$$

where $b = (U_1/U_0)\,\mathrm{d}L/\mathrm{d}x$. Using the experimental value of b ($\simeq 0.078$), equation (1) is in reasonable agreement with the measured distribution $\overline{uv}/U_0^2$ (Fig. 5(a)) while equation (2) yields values of $\overline{v\theta}/U_0T_0$ that are larger than the measurements, the maximum deviation being about 17% near $\eta \simeq 1$. This deviation seems tolerable in view of the uncertainty, equal to about $\pm 11\%$ in $\overline{v\theta}/U_0T_0$ (our estimated uncertainty in $\overline{uv}/U_0^2$ is about $\pm 10\%$). Since the streamwise variation of L is not given by Fabris, it cannot be ascertained whether his measured values of the Reynolds shear stress and lateral heat flux satisfy the conservation of momentum and enthalpy equations.

Distributions of eddy diffusivities, calculated from

$$\nu_T = -\frac{\overline{uv}}{(\partial\bar{U}/\partial y)}$$

$$\nu_{Tt} = -\frac{\overline{(uv)_t}}{(\partial\bar{U}/\partial y)_t}$$

$$\alpha_T = -\frac{\overline{v\theta}}{(\partial\bar{T}/\partial y)}$$

$$\alpha_{Tt} = -\frac{\overline{(v\theta)_t}}{(\partial\bar{T}/\partial y)_t}$$

are plotted in Fig. 6. There is a small region ($0.3 \lesssim \eta \lesssim 0.8$) where the rate of decrease of ν_T/U_0L is sufficiently small for the normalized momentum

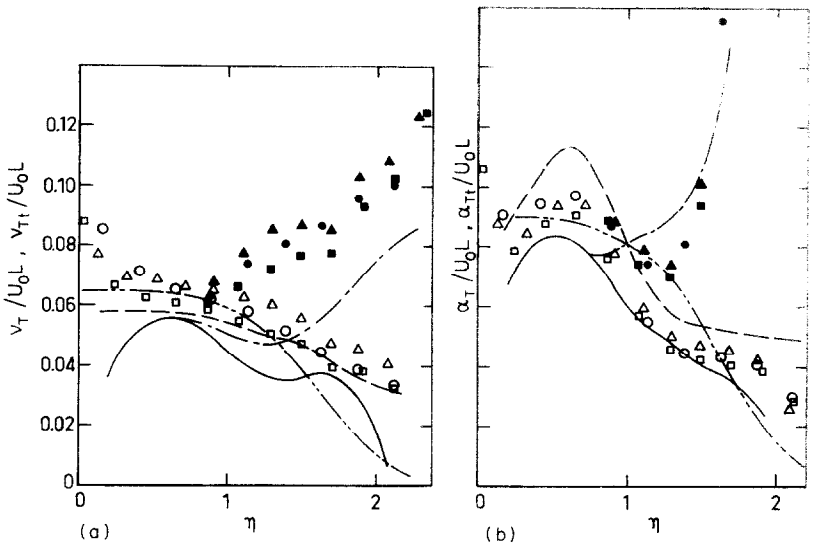

FIG. 6. Turbulent eddy viscosity and eddy diffusivity distributions: (a) turbulent eddy viscosity; (b) turbulent eddy diffusivity. ——— ——: (a) $\nu_T = 0.065\gamma$; (b) $\alpha_T = 0.09\gamma$. Other symbols are as in Fig. 5.

diffusivity to be assumed constant. Outside this range, there is a continuous decrease towards the edge of the wake and a relatively rapid increase as the centreline is approached. The limiting value of ν_T/U_0L at $\eta = 0$, as given by l'Hôpital's rule, is equal to 0.083. The turbulent thermal diffusivity α_T behaves similarly to ν_T near the centreline with a limiting value of 0.076 for α_T/U_0L at $\eta = 0$. However, in contrast to ν_T, α_T is not constant in the range $0.3 \lesssim \eta \lesssim 0.8$ but has in fact a local peak near $\eta = 0.6$ as can also be inferred from Fabris' [7] data. The distributions of ν_T/U_0L and α_T/U_0L estimated using equations (1) and (2) are closely similar to the measurements, the quantitative difference reflecting that in Fig. 5. When averages in only the turbulent zone are considered, ν_{Tt}/U_0L increases for $\eta > 1$ but the increase in α_{Tt}/U_0L, for $\eta \gtrsim 1.3$, is much more pronounced. The conditional distributions of ref. [7] are qualitatively consistent with these trends but the details are significantly different and the magnitudes differ by a maximum of 30%.

Figure 6 clearly indicates that an assumption of constant eddy diffusivity would be of limited use for calculating the mean velocity or the mean temperature. Tennekes and Lumley [17, p. 117] stressed that a constant value of $\nu_T (\equiv \nu_{TC}$ say) is only appropriate near the centreline, while $\nu_T \simeq \gamma\nu_{TC}$ is more appropriate in the intermittent region. Figure 6(a) shows that, in the outer wake, measured values of ν_T/U_0L lie above the distribution corresponding to $\gamma(\nu_{TC}/U_0L)$, with $\nu_{TC}/U_0L = 0.065$. There are also differences (Fig. 6(b)) between measured values of α_T/U_0L and the distribution $\gamma(\alpha_{TC}/U_0L)$, with $\alpha_{TC}/U_0L = 0.09$. Accordingly, we found that calculations of $\bar{U}$ and $\bar{T}$, using the approximations $\nu_T \simeq \gamma\nu_{TC}$ and $\alpha_T = \gamma\alpha_{TC}$, showed departures from measurements. These departures are however smaller than those obtained with the use of a constant eddy diffusivity assumption.

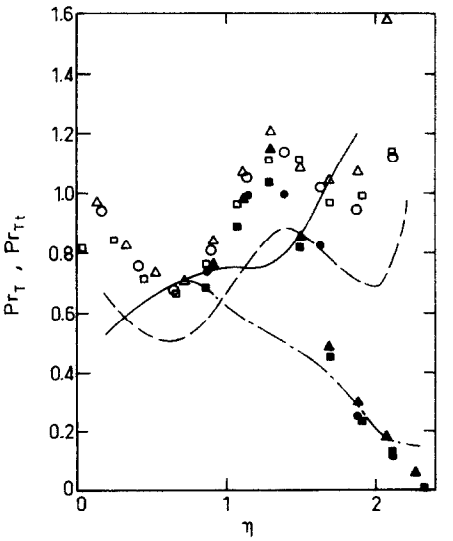

FIG. 7. Turbulent Prandtl number distributions, calculated from ν_T/α_T or ν_{Tt}/α_{Tt}. Symbols are as in Fig. 5.

The shape of the turbulent Prandtl number distribution (Fig. 7) calculated from $Pr_T = \nu_T/\alpha_T$ reflects, of necessity, the behaviour of ν_t and α_t. There is no significant range of η over which Pr_T can be assumed to be constant. Away from the centreline, Pr_T displays a succession of extrema, with minima at $\eta \simeq 0.7$ and 1.8 and a maximum at $\eta \simeq 1.3$. This behaviour cannot be attributed to experimental inaccuracies since these trends were reproducible at all stations and also the experiments at $x/d = 420$ were repeated a number of times; the maximum variation in Pr_T is certainly larger than the experimental uncertainty ($\pm 15\%$) in Pr_T. We inferred this uncertainty, using the propagation of errors, from uncertainties in $\overline{uv}/U_0^2$ ($\simeq \pm 9\%$), $\overline{v\theta}/U_0T_0$ ($\simeq \pm 11\%$); f' ($\simeq \pm 3\%$) and g' ($\simeq \pm 3\%$). We also estimated Pr_T by using the relation

$Pr_T = (\overline{uv}/\overline{v\theta})(\partial\bar{T}/\partial\bar{U})$ and applying least squares fits to the data of $\bar{T}$ vs $\bar{U}$. This approach (e.g. refs. [18, 19]) improved the uncertainty in Pr_T slightly ($\pm 11\%$) but yielded essentially the same distributions for Pr_T as those shown in Fig. 7. The present distribution of the turbulent Prandtl number is in disagreement with the prediction [20], using a second-order closure for heat transfer, of a constant Pr_T in the region $0 \leqslant \eta \lesssim 0.9$. The present results, like those in a turbulent plane jet [21], suggest that there is only a narrow range of η for which Pr_T is substantially less than unity.

The values of Pr_{Tt} (Fig. 7) fall rather rapidly towards the edge of the wake. This trend, which is similar to that observed in ref. [14] in the outer region of a circular jet with a co-flowing stream, is a consequence of $(\overline{v\theta})_t$ being larger than $(\overline{uv})_t$ and g_t' smaller than f_t'. Note that the use of conditional averages, obtained using fluctuations relative to overall means instead of zone averaged means, would further emphasize the decrease in Pr_{Tt} towards the edge of the wake (see, e.g. ref. [14]) as a result of the relatively larger contributions from $\bar{v}_t\bar{\theta}_t$ than from $\bar{u}_t\bar{v}_t$.

CONCLUSIONS

Conventional and conditional results for the velocity and thermal fields of a turbulent wake support self-preservation for the range of x/d covered by the experiment. Distributions of momentum and heat fluxes satisfy approximately the momentum and enthalpy equations and indicate significant variations, across the wake, of turbulent momentum and thermal diffusivities. The resulting conventional Prandtl number distribution is such that a claim of a constant Prandtl number is tenuous, even for a narrow region of the wake. In particular, the Prandtl number within only the turbulent flow zone decreases rapidly near the edges of the wake, implying that the transport of heat is carried out more effectively than that of momentum.

REFERENCES

1. J. C. LaRue and P. A. Libby, Temperature fluctuations in the plane turbulent wake, *Physics Fluids* **17,** 1956–1967 (1974).
2. P. Freymuth and M. S. Uberoi, Structure of temperature fluctuations in the turbulent wake behind a heated cylinder, *Physics Fluids* **14,** 2574–2580 (1971).
3. M. S. Uberoi and P. Freymuth, Spectra of turbulence in wakes behind circular cylinders, *Physics Fluids* **12,** 1359–1363 (1969).
4. A. A. Townsend, The fully developed turbulent wake of a circular cylinder, *Aust. J. Scient. Res.* **2,** 451–468 (1949).
5. W. Rodi, A review of experimental data of uniform density free turbulent boundary layers. In *Studies in Convection* (Edited by B. E. Launder), Vol. 1, pp. 79–165. Academic Press, New York (1975).
6. A. Hariri, P. A. Libby and J. C. LaRue, Similarity solutions and experiment for turbulent wakes, *Physics Fluids* **25,** 1964–1967 (1982).
7. G. Fabris, Conditionally sampled turbulent thermal and velocity fields in the wake of a warm cylinder and its interactions with an equal cool wake, Ph.D. Thesis, Illinois Institute of Technology, Chicago (1974).
8. P. Paranthoen, J. C. Lecordier and C. Petit, The effect of the thermal prong wire interaction on the response of a cold wire in gaseous flow (air, argon, helium), *J. Fluid Mech.* **124,** 457–473 (1982).
9. L. W. B. Browne and R. A. Antonia, Reynolds shear stress and heat flux measurements in a cylinder wake, *Physics Fluids* **29,** 709–713 (1986).
10. M. L. Barsoum, J. G. Kawall and J. F. Keffer, Spanwise structure of the plane turbulent wake, *Physics Fluids* **21,** 157–161 (1978).
11. R. A. Antonia, Conditional sampling in turbulence measurement, *Ann. Rev. Fluid Mech.* **13,** 131–156 (1981).
12. R. W. Bilger, R. A. Antonia and K. R. Sreenivasan, Determination of intermittency from the probability density function of a passive scalar, *Physics Fluids* **19,** 1471–1474 (1976).
13. G. Fabris, Conditional sampling study of the turbulent wake of a cylinder. Part 1, *J. Fluid Mech.* **94,** 673–709 (1979).
14. R. A. Antonia, A. Prabhu and S. W. Stephenson, Conditionally sampled measurements in a heated turbulent jet, *J. Fluid Mech.* **72,** 455–480 (1975).
15. S. F. Ali and L. S. G. Kovasznay, Approach to self-preservation in a heated wake behind a flat plate, ASME Paper 74-WA/HT-35 (1974).
16. H. E. Fiedler, On turbulence structure and mixing mechanism in free turbulent shear flows. In *Turbulent Mixing in Non-reactive and Reactive Flows* (Edited by S. N. B. Murthy), pp. 381–409. Plenum, New York (1975).
17. H. Tennekes and J. L. Lumley, *A First Course in Turbulence*. MIT Press, Cambridge, Massachusetts (1972).
18. J. Blom, An experimental determination of the turbulent Prandtl number in a developing temperature boundary layer, Ph.D. Thesis, Technical University, Eindhoven (1970).
19. M. M. Pimenta, R. J. Moffat and W. M. Kays, The structure of a boundary layer on a rough wall with blowing and heat transfer, *J. Heat Transfer* **101,** 193–198 (1979).
20. B. E. Launder and D. S. A. Samaraweera, Application of a second-moment turbulence closure to the heat and mass transport in thin shear flows—I. Two-dimensional transport, *Int. J. Heat Mass Transfer* **22,** 1631–1643 (1979).
21. L. W. B. Browne and R. A. Antonia, Measurements of turbulent Prandtl number in a plane jet, *J. Heat Transfer* **105,** 663–665 (1983).

NOMBRE DE PRANDTL CONVENTIONNEL ET CONDITIONNEL DANS UN SILLAGE PLAN TURBULENT

Résumé—Des mesures conventionnelles et conditionnelles de quelques grandeurs de turbulence, et particulièrement du nombre de Prandtl turbulent, sont présentées pour la région presque auto-entretenue du sillage d'un cylindre circulaire faiblement chauffé. Pour vérifier que les mesures sont faites effectivement dans cette région et aussi que les mesures sont précises, on utilise trois positions dans le sillage. L'identification des régions turbulentes dans la partie extérieure du sillage est basée sur le comportement de la fonction densité de probabilité de la fluctuation de température. Des distributions conventionnelles des diffusivités de quantité de mouvement et de chaleur varient très fortement dans la partie externe du sillage. Cette variation n'est pas réduite quand on considère seulement les moyennes de la zone turbulente. Le nombre de Prandtl turbulent varie significativement dans la zone turbulente de l'écoulement.

HERKÖMMLICHE UND BEDINGTE PRANDTL-ZAHL IN EINEM TURBULENTEN, EBENEN NACHLAUFGEBIET

Zusammenfassung—Herkömmliche und bedingte Messungen von verschiedenen Turbulenzgrößen, insbesondere der turbulenten Prandtl-Zahl, werden für die fast-selbsterhaltende Region des schwach beheizten Nachlaufgebietes eines Kreiszylinders vorgestellt. Um zu überprüfen, ob die Messungen tatsächlich in der selbsterhaltenden Region durchgeführt wurden, und um die Meßgenauigkeit zu überprüfen, wurde an drei Stellen in der Abströmung gemessen. Die turbulenten Bereiche am äußeren Rand der Abströmung wurden mit Hilfe der Wahrscheinlichkeitsdichte der Temperaturschwankungen erkannt. Die herkömmliche Verteilung des turbulenten Wärme- und Impulstransports schwankt erheblich im äußeren Teil der Abströmung. Diese Schwankung läßt sich durch Mittelwertbildung in der turbulenten Zone allein nicht verringern. Die turbulente Prandtl-Zahl schwankt im turbulenten Bereich der Strömung erheblich.

СТАНДАРТНЫЕ И УСЛОВНО ВЫБОРОЧНЫЕ ЧИСЛА ПРАНДТЛЯ ДЛЯ ТУРБУЛЕНТНОГО ПЛОСКОГО СЛЕДА

Аннотация—Приводятся стандартные и условно выборочные измерения некоторых турбулентных величин и, в частности, числа Прандтля для автомодельной области слабо нагретого следа за круглым цилиндром. Чтобы подтвердить автомодельность области, где выполнены измерения, и проверить их точность, были выбраны три сечения следа. Идентификация турбулентности во внешней части следа основана на поведении функции распределения вероятностей температурных пульсаций. Показано, что обычно измеренные значения коэффициентов турбулентной диффузии, количества движения и тепла претерпевают значительное изменение во внешней части следа. Эти изменения не уменьшаются при определении коэффициентов только для турбулентных участков реализаций сигналов (обусловленное осреднение). В чисто турбулентной части следа турбулентное число Прандтля изменяется значительно.